Available online at www.sciencedirect.com
ScienceDirect
Journal of Molecular Graphics and Modelling 26 (2008) 1014–1019
Journal of Molecular Graphics and Modelling
www.elsevier.com/locate/JMGM

Localization and visualization of excess chemical potential in statistical mechanical integral equation theory 3D-HNC-RISM

Qi-Shi Du [a,b,*], Peng-Jun Liu [b], Ri-Bo Huang [a,c]

[a] Key Laboratory of Subtropical Bioresource Conservation and Utilization, Guangxi University, Nanning, Guangxi 530004, China
[b] Department of Chemistry, Hainan Normal University, Haikou, Hainan 571158, China
[c] Guangxi Academy of Sciences, 98 Daling Road, Nanning, Guangxi 530004, China

Received 2 March 2007; received in revised form 23 August 2007; accepted 25 August 2007
Available online 31 August 2007

Abstract

In this study the excess chemical potential of the integral equation theory, 3D-RISM-HNC [Q. Du, Q. Wei, J. Phys. Chem. B 107 (2003) 13463–13470], is visualized in three-dimensional form and localized at interaction sites of solute molecule. Taking the advantage of reference interaction site model (RISM), the calculation equations of chemical excess potential are reformulized according to the solute interaction sites *s* in molecular space. Consequently the solvation free energy is localized at every interaction site of solute molecule. For visualization of the 3D-RISM-HNC calculation results, the excess chemical potentials are described using radial and three-dimensional diagrams. It is found that the radial diagrams of the excess chemical potentials are more sensitive to the bridge functions than the radial diagrams of solvent site density distributions. The diagrams of average excess chemical potential provide useful information of solute–solvent electrostatic and van der Waals interactions. The local description of solvation free energy at active sites of solute in 3D-RISM-HNC may broaden the application scope of statistical mechanical integral equation theory in solution chemistry and life science.

Keywords: Solvation free energy; Integral equation theory; 3D-RISM-HNC; Statistical mechanics; Visual representation

1. Introduction

The solvent effects play an important role in many research fields of chemistry and life science. Quantitative evaluation of solvation free energy is of the main determinant quantities in the study of molecular conformation and association of biomolecules, such as proteins and polynucleotides. Solvation free energy constitutes an important, but difficult-to-find quantity, posing a challenge to computational chemists. The reference interaction site model (RISM) integral equation theory has received a large amount of interest over the past three decades as a means to calculate the solvation free energy surrounding a solute molecule, as described by radial distribution functions of the solvent site densities $\langle \Delta\rho_\alpha(\mathbf{r})\rangle$ [1–9]. Still more importantly, by employing the hypernetted chain (HNC) closure relation, an expression has been derived for the solvation free energy as a function of these solvent distributions [10–15].

The unique merit of three-dimensional RISM is that it describes the solvation structure surrounding a solute molecular space by solvent site density distribution functions $\langle \Delta\rho_\alpha(\mathbf{r})\rangle$. In the 3D-RISM-HNC approach, the site densities $\langle \Delta\rho_\alpha(\mathbf{r})\rangle$ of solvent molecule are the foundational quantities and all other physical properties of solution are described through the solvent site densities. The formulization of excess chemical potentials has been provided by several authors [9,15–18]. In many cases we do not only want to know the total solvation free energy in solution, but also want to know the solvation structure and the solvation free energies at some active sites in solute molecular structure. For example, the local solvation free energy in active pocket of protease is most interesting in protein chemistry for us, and we want to calculate the docking free energy between ligand and its bioreceptor in the active pocket for rational drug design.

Taking the advantage of reference interaction site model (RISM), in this study we reformulize the calculation equations of excess chemical potential according to the solute interaction

* Corresponding author at: Key Laboratory of Subtropical Bioresource Conservation and Utilization, Guangxi University, Nanning, Guangxi 530004, China. Tel.: +86 771 327 0730.
E-mail address: qishi_du@yahoo.com.cn (Q.-S. Du).

1093-3263/$ – see front matter
doi:10.1016/j.jmgm.2007.08.007

sites s at point $\mathbf{r}$ in molecular space $\langle \Delta\mu_s(\mathbf{r})\rangle$. The goal of this study is to provide a way for the localization and visualization of the excess chemical potential in 3D-RISM-HNC through two examples, *N*-methyl amine (NMA) and ethanol. Although these two molecules are very small comparing with biomolecules, however, the 3D-RISM-HNC approach and the methods provided in this study can be applied in part of macromolecules easily, such as the active pocket of proteins, and to study the excess chemical potential in active sites of proteins.

2. Theory and method

The formulization of 3D-RISM-HNC has been well established in previous works by several authors [9,15–18]. Here we reformulize the equations for localization and visualization of excess chemical potential in 3D-RISM-HNC. The fundamental quantities in RISM for obtaining thermodynamic properties are the reduced average densities $\langle \rho_\alpha(\mathbf{r})\rangle$ of solvent interaction sites. By convention, in this study the Greek letter α is for the solvent interaction sites and the Roman letter s is for the solute interaction sites, respectively. In the 3D-RISM-HNC integral equation theory, average densities $\langle \rho_\alpha(\mathbf{r})\rangle$ are computed from the following HNC iterative closure:

$$h_\alpha(\mathbf{r}) = \mathrm{e}^{[-\beta U_\alpha(\mathbf{r}) + h_\alpha(\mathbf{r}) - c_\alpha(\mathbf{r}) - b_\alpha(\mathbf{r})]} - 1 \tag{1}$$

where $h_\alpha(\mathbf{r}) = \langle \rho_\alpha(\mathbf{r})\rangle/\bar{\rho} - 1$ is the solute–solvent site correlation function and $c_\alpha(\mathbf{r})$ is the solute–solvent direct correlation function defined by

$$\bar{\rho} h_\alpha(\boldsymbol{r}) = \sum_\gamma c_\gamma * \chi_{\gamma\alpha}(\boldsymbol{r}) \tag{2}$$

where $\chi_{\gamma\alpha}(\mathbf{r})$ is the solvent susceptibility response function of pure liquid, and the symbol * represents a special convolution. The function $b_\alpha(\mathbf{r})$ in Eq. (1) is the bridge function of interaction site α in solvent molecule. The interaction potential $U_\alpha(\mathbf{r})$ from the solvent site α is represented by a sum of radially symmetric Lennard–Jones equations (6)–(12), which describes the non-polar van der Waals interactions, and Coulomb electrostatic potential equation centered on the interaction site s of solute,

$$U_\alpha(\mathbf{r}) = \sum_s U_{\alpha s}^{(\mathrm{LJ})}(\mathbf{r}) + \sum_s U_{\alpha s}^{(\mathrm{elec})}(\mathbf{r}) \tag{3}$$

with

$$U_{\alpha s}^{(\mathrm{LJ})}(\mathbf{r}) = 4\varepsilon_{\alpha s}\left[\left(\frac{\sigma_{\alpha s}}{|\mathbf{r}-\mathbf{r}_s|}\right)^{12} - \left(\frac{\sigma_{\alpha s}}{|\mathbf{r}-\mathbf{r}_s|}\right)^{6}\right] \tag{4}$$

and

$$U_{\alpha s}^{(\mathrm{elec})}(\mathbf{r}) = \frac{q_\alpha q_s}{|\mathbf{r}-\mathbf{r}_s|} \tag{5}$$

where $\varepsilon_{\alpha s}$, $\sigma_{\alpha s}$, q_α, and q_s are the L–J parameters and atomic charges, respectively. The parameters used in 3D-RISM-HNC are commonly taken from the molecular mechanical force fields, such as AMBER [19], CHARMM [20] and OPLS [2].

The excess chemical potential on site s of solute is the sum of non-polar and electrostatic free energy contributions. For numerical convenience, the two parts of excess chemical potential are evaluated by integration over scaling factor λ [9,11,17] of L–J radius, $\lambda\sigma_{\alpha s}$, and of the solute atomic charges, λq_s, from 0 to 1, respectively,

$$\langle \Delta\mu_s^{(\mathrm{np})}(\mathbf{r})\rangle = \int_0^1 \mathrm{d}\lambda \sum_\alpha \frac{\partial U_{\alpha s}^{(\mathrm{LJ})}(\mathbf{r};\lambda)}{\partial\lambda} \langle \rho_\alpha(\mathbf{r})\rangle \tag{6}$$

and

$$\langle \Delta\mu_s^{(\mathrm{elec})}(\mathbf{r})\rangle = \int_0^1 \mathrm{d}\lambda \sum_\alpha \frac{\partial U_{\alpha s}^{(\mathrm{elec})}(\mathbf{r};\lambda)}{\partial\lambda} \langle \rho_\alpha(\mathbf{r})\rangle \tag{7}$$

The total average excess chemical potential $\langle \Delta\mu(\mathbf{r})\rangle$ is obtained by adding these two parts,

$$\langle \Delta\mu_s(\mathbf{r})\rangle = \langle \Delta\mu_s^{(\mathrm{np})}(\mathbf{r})\rangle + \langle \Delta\mu_s^{(\mathrm{elec})}(\mathbf{r})\rangle \tag{8}$$

In Eqs. (6)–(8), the average excess chemical potential $\langle \Delta\mu_s(\mathbf{r})\rangle$ is formulized according to the solute interaction sites s and at point $\mathbf{r}$ in space, which describe the local solvation free energies at interaction sites of solute. In this way we can plot the radial and three-dimensional diagrams of average excess chemical potentials for solute interaction sites, and also provide local description for solvation free energy in the vicinity where we are interested.

In Eq. (1), the potential energy function $U_\alpha(\mathbf{r})$ plays an important role for the accuracy of calculation results. However, using accurate and sophisticated potential function (e.g. quantum mechanical potential functions) is very difficult and it may lose the merit of simplicity and efficiency in 3D-RISM-HNC approach. One method to improve the accuracy of 3D-RISM-HNC is the bridge functions $b_\alpha(\mathbf{r})$ for each interaction site of solvent molecule [9,17,18], which are the remediation terms for potential function $U_\alpha(\mathbf{r})$. The bridge function $b_\alpha(\mathbf{r})$ has well-defined formal diagrammatic structure in the theory of liquids [4]. The bridge functions play the role of effective potentials, which are adjusted empirically in this study to improve the accuracy of the calculation results. Water molecule has three interaction sites, one oxygen atom and two hydrogen atoms. The hydrogen bridge function $b_\mathrm{H}(\mathbf{r})$ is simply a remedial term for the L–J interaction function,

$$b_\mathrm{H}(\mathbf{r};\lambda) = -\ln[\omega_\mathrm{OH} * \mathrm{e}^{[-\beta U_\mathrm{O}^{(\mathrm{LJs})}(\mathbf{r};\lambda)]}] \tag{9}$$

and ω_OH is the site–site intramolecular correlation function,

$$\omega_\mathrm{OH} = \frac{\delta(|\mathbf{r}| - l_\mathrm{OH})}{4\pi l_\mathrm{OH}^2} \tag{10}$$

where the symbol * represents a three-dimensional convolution. The hydrogen bridge function describes the repulsive interaction of solute–water in short distance. Because there is no repulsive branch in potential equation at short distance for hydrogen, if the water TIP3 model [21] is used.

Table 1
Solvation of alkanes (All energies are in kcal/mol)

	Molecule				
	Methane	Ethane	Propane	Butane	Pentane
$\Delta\mu_{cal}$[a]	2.084	1.827	2.024	2.136	2.292
$\Delta\mu_{exp}$[b]	2.00	1.83	1.96	2.08	2.33

[a] The parameter a_0 is 0.397 in oxygen bridge function Eq. (12).
[b] From Ref. [26].

In addition to the hydrogen bridge function, it is also important to introduce an oxygen bridge function $b_O(\mathbf{r})$ of water for accurate solvation free energies. The value of the solvent density in contact with the solute is slightly overestimated even close to non-polar groups, which yields systematically too positive excess free energies $\langle\Delta\mu^{(np)}\rangle$. Previous studies [17,18] of the bridge function showed that the oxygen bridge function plays the role of an effective repulsive potential depending on radius of the solute molecule [22–25]. For simplicity, we assume that the water oxygen bridge function consists of a superposition of rapidly decaying radial functions centered on the solute site s, as defined by the following equations:

$$b_O(\mathbf{r};\lambda) = \sum_s A_s\, e^{-(|\mathbf{r}-\mathbf{r}_s|-\lambda\sigma_{Os}(\sigma_{Os}/y_0))/y} \tag{11}$$

where the amplitude A_s takes the form

$$A_s = a_0 \frac{\lambda\sigma_{Os}/y_0}{1+\lambda} \tag{12}$$

In Eqs. (9)–(12) the parameter λ is a scaling factor. The parameter y in Eq. (11) represents the decay length of the exponential function. Since the bridge functions of simple liquids are effective in short range, y is assigned a value of 0.50 Å. The parameter y_0 controls how much magnitude of the amplitude A_s varies as a function of the size of the solute particle. It was assigned a value of 2.8 Å, corresponding to the average distance between two oxygen atoms in liquid water. The amplitude parameter a_0 controls the overall magnitude of oxygen function and has a significant influence on the calculated free energies. The value of a_0 is optimized and the best value of a_0 is 0.397, which gives the calculation results of excess chemical potentials very close to the experimental values (see Table 1 and Fig. 1).

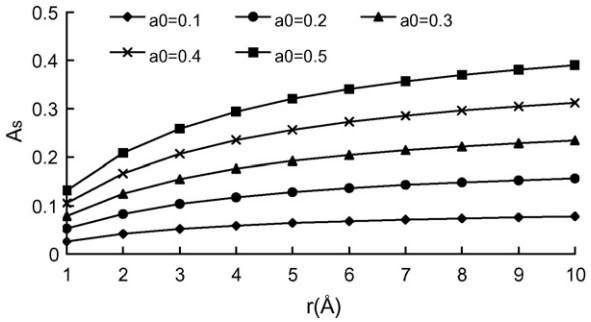

Fig. 1. The effects of a_0 and radius σ_{Os} on the amplitude A_s of the oxygen bridge function. y_0 = 2.8 Å, λ = 1.

3. Calculation results

The average densities of solvent interaction sites, $\langle\rho_\alpha(\mathbf{r})\rangle$, are the fundamental quantities for thermodynamic properties of solution in the integral equation theory of statistical mechanics. In 3D-RISM-HNC, $\langle\rho_\alpha(\mathbf{r})\rangle$ can be examined by radial distribution diagrams [17,18] of solvent interaction sites and

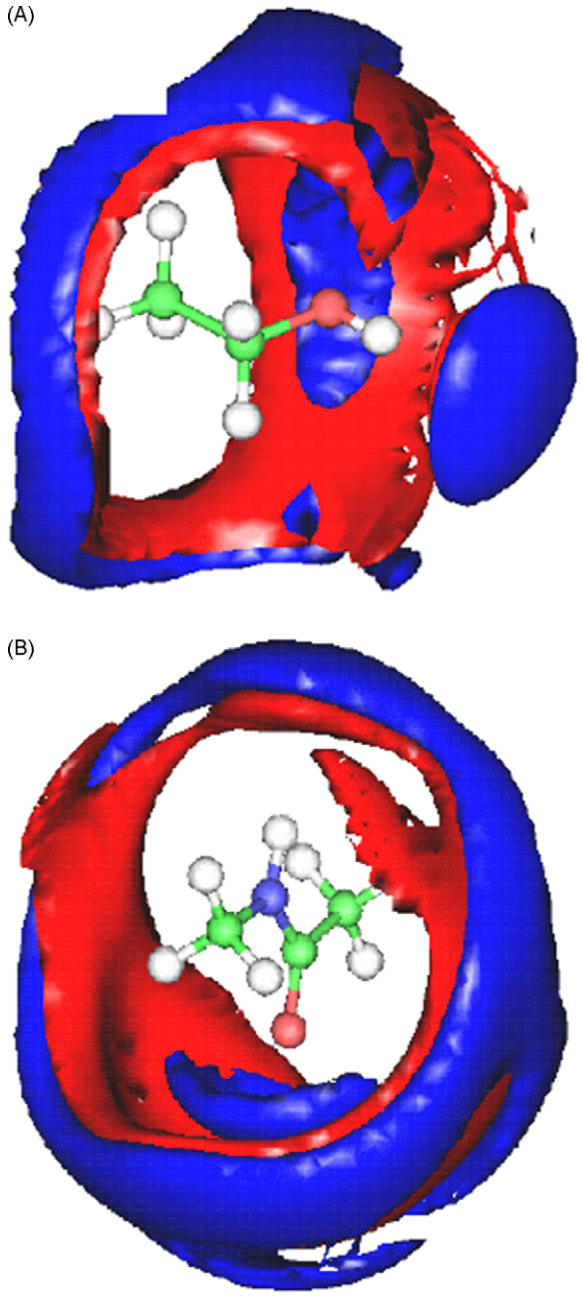

Fig. 2. (A) Three-dimensional distributions of $\langle\rho_O(\mathbf{r})\rangle$ and $\langle\rho_H(\mathbf{r})\rangle$ surrounding the ethanol molecule. The red represents oxygen and the blue represents hydrogen. There is higher oxygen density $\langle\rho_O(\mathbf{r})\rangle$ in the front of H and higher hydrogen density $\langle\rho_H(\mathbf{r})\rangle$ in the outside of O in the hydroxy group (OH). (B) Three-dimensional distributions of $\langle\rho_O(\mathbf{r})\rangle$ and $\langle\rho_H(\mathbf{r})\rangle$ surrounding the NMA molecule. The red represents oxygen and blue represents $\langle\rho_H(\mathbf{r})\rangle$. There is higher hydrogen density $\langle\rho_H(\mathbf{r})\rangle$ in the front of O in (C═O) group and higher oxygen density $\langle\rho_O(\mathbf{r})\rangle$ in the front of H in NH group. (B) Adapted from Fig. 2 of Ref. [18] with permission.

by three-dimensional figures around the solute molecule. In Fig. 2 we present the three-dimensional density distributions of oxygen $\langle\rho_O(\mathbf{r})\rangle$ and hydrogen $\langle\rho_H(\mathbf{r})\rangle$ of the water molecule around NMA (*N*-methyl amine) and ethanol molecule. The red represents oxygen density and the blue represents the hydrogen density. In Fig. 2(A), in the front of H(OH) of polar atomic group OH of ethanol, there is higher density of water oxygen $\langle\rho_O(\mathbf{r})\rangle$ and in the outside of O(OH) there is higher density of water hydrogen density $\langle\rho_H(\mathbf{r})\rangle$. The higher densities of water oxygen and hydrogen describe the orientation of water molecules and indicate the hydrogen bond between water and ethanol. On the non-polar part, i.e., the hydrocarbon chain —C_2H_5, the densities of oxygen and hydrogen of water have no change comparing with bulk water. Fig. 2(B) is the water oxygen and hydrogen density distributions in three-dimensional space surrounding NMA. In Fig. 2(B), near the polar atomic groups NH and C=O of NMA we find big changes of densities of oxygen and hydrogen of water. There is higher water hydrogen density in the front of O in C=O group, however, in the front of H in NH group there is higher water oxygen density, indicating the formation of hydrogen bonds. Three-dimensional figures give a visual representation of solvent molecules surrounding the solute molecule and also indicate the positions of hydrogen bonds.

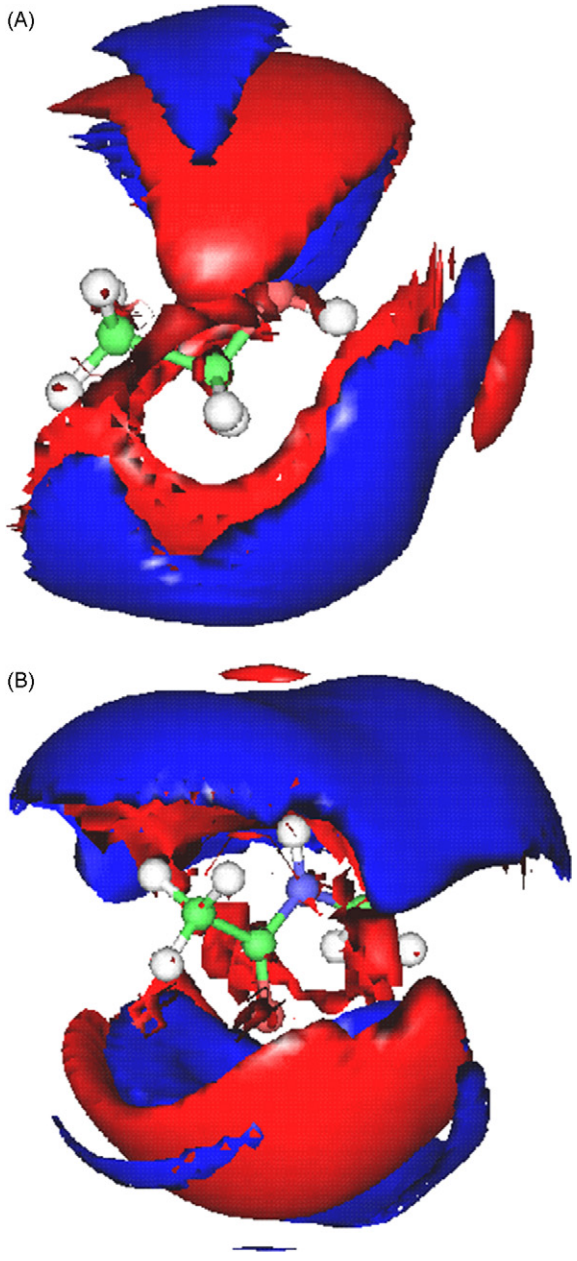

Fig. 3. (A) Three-dimensional distribution of the excess chemical potential surrounding the ethanol molecule in water solution. The red is the positive excess chemical potential $\langle\Delta\mu^+(\mathbf{r})\rangle$ and blue is the negative excess chemical potential $\langle\Delta\mu^-(\mathbf{r})\rangle$. (B) Three-dimensional distribution of excess chemical potential surrounding NMA in liquid water. The red is the positive excess chemical potential $\langle\Delta\mu^+(\mathbf{r})\rangle$ and the blue is the negative excess chemical potential $\langle\Delta\mu^-(\mathbf{r})\rangle$.

The excess chemical potential $\langle\Delta\mu_\alpha(\mathbf{r})\rangle$ is an important property in 3D-RISM-HNC and is used to illustrate many chemical phenomena. According to the Eq. (8), we construct the diagrams of three-dimensional distributions of excess chemical potentials $\langle\Delta\mu(\mathbf{r})\rangle$ in the space around the solute molecule. In performing the calculations, the scaling factor λ is divided into 10 fragments with an increment of 0.1, from 0 to 1.0. Fig. 3 shows the three-dimensional distributions of excess chemical potentials in the molecular spaces of ethanol and NMA. The red color represents the positive excess chemical potential and blue color is the negative chemical potential. Outside of O(OH) in ethanol, the color is the blue–red–blue. It means negative–positive–negative change of the excess chemical potential $\langle\Delta\mu(\mathbf{r})\rangle$ in this vicinity of O(OH). On the other hand, in the front of H(OH), the change of the excess chemical potential $\langle\Delta\mu(\mathbf{r})\rangle$ is positive–negative–positive (red–blue–red).

The hydrogen bridge function $b_H(\mathbf{r})$ and oxygen bridge functions $b_O(\mathbf{r})$ make significant improvement on excess

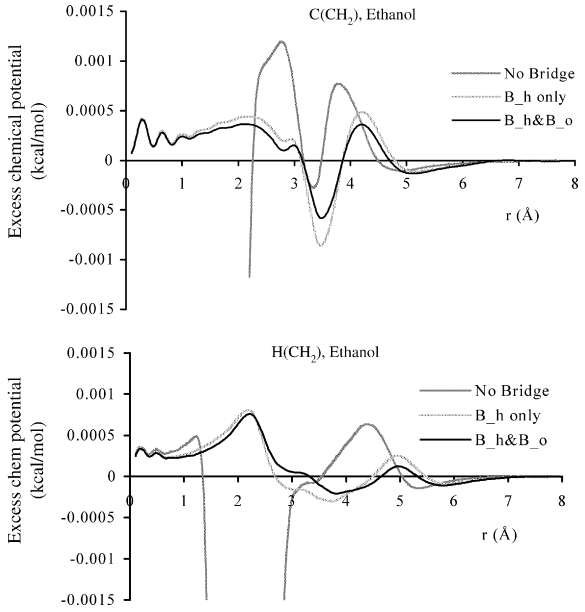

Fig. 4. The radial average excess chemical potential $\langle\Delta\mu(\mathbf{r})\rangle$ around the $C(CH_2)$ and $H(CH_2)$ of the ethanol molecule, calculated with and without hydrogen and oxygen bridge functions in 3D-RISM-HNC approach.

chemical potential $\langle \Delta\mu(\mathbf{r})\rangle$. The effects of bridge functions can be found directly by checking the excess chemical potential $\langle \Delta\mu_\alpha(\mathbf{r})\rangle$ based on Eq. (8). The effects of bridge functions $b_O(\mathbf{r})$ and $b_H(\mathbf{r})$ are shown in the figures of radial distributions of excess chemical potentials $\langle \Delta\mu(\mathbf{r})\rangle$ on each interaction site of the solute molecule. Figs. 4–6 are the radial average excess chemical potential $\langle \Delta\mu(\mathbf{r})\rangle$ around the interaction sites of ethanol and NMA molecules in liquid water, calculated with and without hydrogen and oxygen bridge functions $b_O(\mathbf{r})$ and $b_H(\mathbf{r})$. Observation from Figs. 4–6 we find that if no hydrogen function $b_H(\mathbf{r})$ and oxygen bridge functions $b_O(\mathbf{r})$ are used, near the nuclear centers of negatively charged atoms $C(CH_2)$, $C(CH_3)$, and O(OH), there are infinite negative excess chemical potentials. For positive charged atoms, $H(CH_2)$, $H(CH_3)$, and H(OH), there are very deep wells of excess chemical potentials between 1 and 2 Å. Without bridge functions 3D-RISM-HNC approach cannot give even qualitative evaluation for thermodynamic properties of solution. Use of the hydrogen bridge function $b_H(\mathbf{r})$ eliminates these unreasonable peaks of the excess chemical potentials and makes the curves more reasonable. The oxygen bridge function $b_O(\mathbf{r})$ gives further improvement for the calculation results of the excess chemical potentials. For polar atoms, like O and H in OH group, on the diagrams of radial distribution of the excess chemical potentials, there is a deep potential well between 2 and 3 Å, and a peak between 3 and 4 Å which are caused by electrostatic interactions. The potential well of the van der Waals interaction between 4 and 5 Å (Fig. 5) is very shallow. For non-polar atoms in CH_3 group, the electrostatic interaction is not as strong as polar atoms, however, the potential well of van der Waals interaction is bigger than that of polar atoms (Fig. 6).

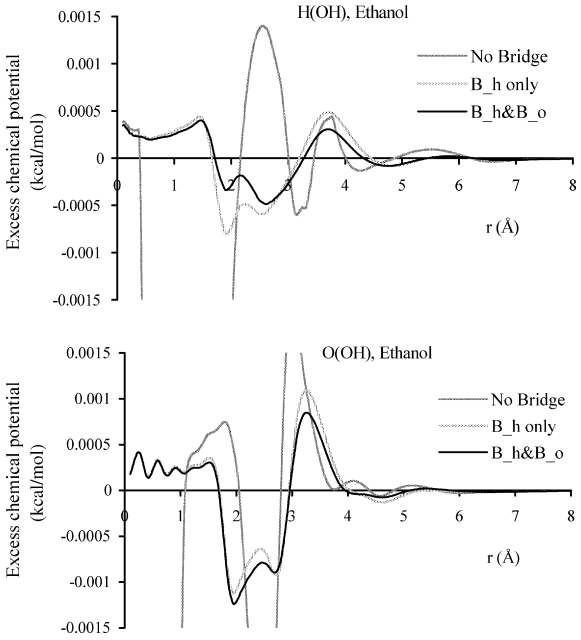

Fig. 5. The radial average excess chemical potential $\langle \Delta\mu(\mathbf{r})\rangle$ around the H(OH) and O(OH) of the ethanol molecule, calculated with and without hydrogen and oxygen bridge functions in 3D-RISM-HNC approach.

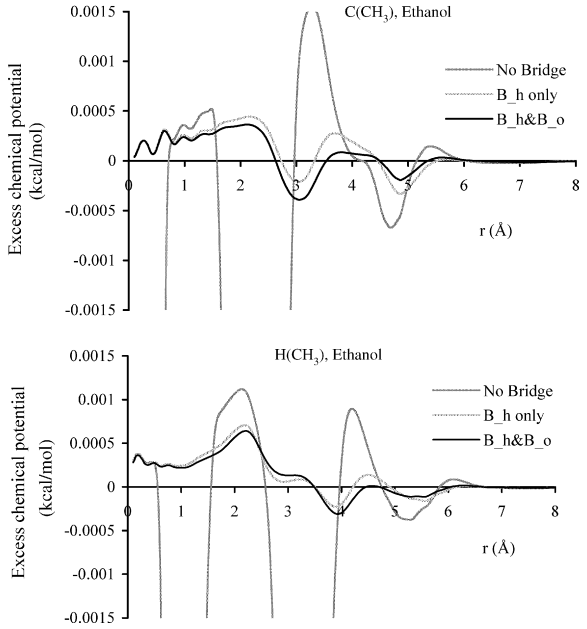

Fig. 6. The radial average excess chemical potential $\langle \Delta\mu(\mathbf{r})\rangle$ around the $C(CH_3)$ and $H(CH_3)$ of the ethanol molecule, calculated with and without hydrogen and oxygen bridge functions in 3D-RISM-HNC approach.

4. Summary and conclusion

In this study we have presented an expression for the localization and visualization of solvation free energies in 3D-RISM-HNC approach. The integral equation theory provides the average densities of solvent interaction sites $\langle \rho_\alpha(\mathbf{r})\rangle$ in three dimensions around a complex solute molecule, which is the foundational physical quantity. Taking the advantage of reference interaction site model (RISM), the calculation equations of excess chemical potential $\langle \Delta\mu_s(\mathbf{r})\rangle$ are expressed at the interaction sites of solute molecule. In this way the excess chemical potentials are localized at interaction sites of solute and visualized using radial and three-dimensional diagrams. The radial and three-dimensional diagrams of excess chemical potentials of the two examples (NMA and ethanol) revealed the solvation information of van der Waals interaction and electrostatic interaction between solvent and solute molecules that cannot be found in the corresponding diagrams of solvent site density distributions. The two examples proved that the radial and three-dimensional diagrams of excess chemical potentials are more effective than the diagrams of solvent site distributions for examining the effects of oxygen bridge function $b_O(\mathbf{r})$ and hydrogen bridge function $b_H(\mathbf{r})$.

The localization method for excess chemical potential $\langle \Delta\mu_s(\mathbf{r})\rangle$ of solute interaction sites, provided in this study, extended the application scope of 3D-RISM-HNC. The 3D-RISM-HNC approach can be applied to study whole or part of biomolecular system, e.g. proteins and polynucleotides. Some examples can be found in references [27,28]. The excess chemical potential in catalytic active pockets of proteases is a possible research field of the method developed in this study. The localization and visualization of excess chemical potential in the active pocket can provide useful insight into

the ligand–receptor interaction. The methodology developed in this study can also be applied to other thermodynamic properties in 3D-RISM-HNC approach.

Acknowledgements

The calculations of this study were completed in the University of Montreal under the supervision of Prof. Benoit Roux in 2000 and the paper was composed in China in 2006. Authors thank Prof. Roux very much for his thoughtful discussion and instruction. In China this work was supported by the Chinese National Science Foundation (NSFC) and by Hainan Natural Science Foundation (HNSF) under the contract number 60505.

References

[1] D. Chandler, J.D. McCoy, S.J. Singer, J. Chem. Phys. 85 (1986) 5971.
[2] C.J. Cramer, D.G. Truhlar, in: K.B. Lipkowitz (Ed.), Reviews in Computational Chemistry, VCH, New York, 1995.
[3] C.-L. Brooks III, M. Karplus, B.M. Pettitt, in: I. Prigogine, S.A. Rice (Eds.), Advances in Chemical Physics, vol. LXXI, John Wiley & Sons, New York, 1988.
[4] M.P. Allen, D.J. Tildesley, Computer Simulation of Liquids, Oxford Science Publications, Clarendon Press, Oxford, 1989.
[5] (a) F. Hirata, P.J. Rossky, Chem. Phys. Lett. 83 (1981) 329;
(b) F. Hirata, B.M. Pettitt, P.J. Rossky, J. Chem. Phys. 77 (1982) 509.
[6] P.J. Rossky, H.L. Friedman, J. Chem. Phys. 72 (1980) 5694.
[7] (a) H.C. Andersen, D. Chandler, J. Chem. Phys. 57 (1972) 1918;
(b) D. Chandler, H.C. Andersen, J. Chem. Phys. 57 (1972) 1930.
[8] J.P. Hansen, I.R. McDonald, Theory of Simple Liquids, 2nd ed., Academic, London, 1986.
[9] H. Freedman, T.N. Truong, J. Chem. Phys. 121 (2004) 2187.
[10] T. Morita, K. Hiroike, Prog. Theor. Phys. 23 (1960) 1003.
[11] S.J. Singer, D. Chandler, Mol. Phys. 55 (1985) 621.
[12] D.A. Zichi, P.A. Rossky, J. Chem. Phys. 84 (1985) 1712.
[13] M. Orozco, F.J. Luque, Chem. Rev. 100 (2000) 4187.
[14] H.A. Yu, M. Karplus, J. Chem. Phys. 89 (1988) 2366.
[15] H.A. Yu, B. Roux, M. Karplus, J. Chem. Phys. 92 (1990) 5020.
[16] A. Agarwal, F. Brown, M.R. Reddy, in: M.R. Reddy, M.D. Erion (Eds.), Free Energy Calculations in Rational Drug Design, Kluwer Academic/Plenum, New York, 2001.
[17] Q. Du, D. Beglov, B. Roux, J. Phys. Chem. B 104 (2000) 796.
[18] Q. Du, Q. Wei, J. Phys. Chem. B 107 (2003) 13463–13470.
[19] S.T. Weiner, P.A. Kollman, D.A. Case, U.C. Singh, C. Ghio, G. Alagona, S. Profeta, P. Weiner, J. Am. Chem. Soc. 106 (1984) 765.
[20] W.L. Jorgensen, J. Tirado-Rives, J. Am. Chem. Soc. 110 (1988) 1657.
[21] W.L. Jorgensen, J. Chandrasekhar, J.D. Madura, R.W. Impey, M.J. Klein, J. Chem. Phys. 79 (1983) 926.
[22] F. Lado, Phys. Rev. A 8 (1973) 2548.
[23] F. Lado, S.M. Foiles, N.W. Ashcroft, Phys. Rev. A 28 (1983) 2374.
[24] S.M. Foiles, N.W. Ashcroft, S.M. Reatto, J. Chem. Phys. 81 (1984) 6140.
[25] S.M. Foiles, N.W. Ashcroft, S.M. Reatto, J. Chem. Phys. 80 (1984) 4441.
[26] S. Cabani, P. Gianni, V. Mollica, L. Lepori, J. Sol. Chem. 10 (1981) 563.
[27] A. Yethiraj, J. Chem. Phys. 116 (2002) 5910–5911.
[28] A. Masunov, T. Lazaridis, J. Am. Chem. Soc. 125 (2003) 1722–1730.